

N ISMIRM-ESMRMB 2022 **NEWSLETTER**

NUKEM Isotopes GmbH

Vol. # 4

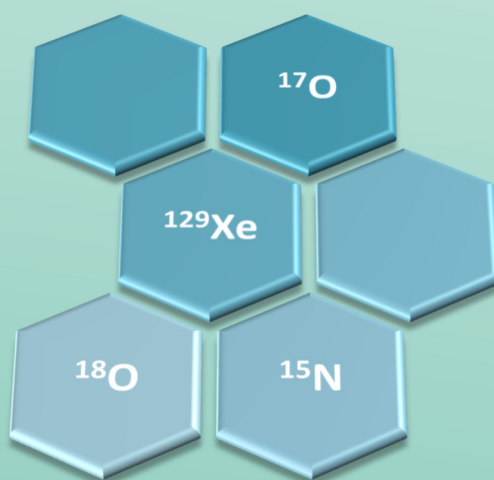
Product brochures of our isotopes

Oxygen-17 ISMIRM abstracts

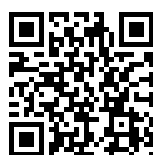
And much more...

Highlight

The O-17 expert team of the German Cancer Research Center, published the first $^{17}\text{O}_2$ study with 10 glioma patients in RSNA Radiology Journal (see page 10) in 2020.



[Contact us](#)



[Company Video](#)



www.nukemisotopes.de

<i>Company Information</i>	1
<i>Company History</i>	2
<i>Our main imaging products</i>	4
<i>Oxygen-17 product information</i>	5
Oxygen-17 in the form of Oxygen gas	5
Oxygen-17 in the form of water	6
Oxygen-17 in the form of D-Glucose	7
<i>Xenon-129 product information</i>	8
Xenon-129 in the form of pure gas.....	8
<i>Nitrogen-15 & Oxygen-18</i>	9
Nitrogen-15 in the form of gas and salts for medical and agricultural applications	9
Oxygen-18 in the form of water for medical applications	9
<i>Highlight (from 2020)</i>	10
Quantitative Dynamic Oxygen-17 MRI at 7.0 T for the Cerebral Oxygen Metabolism in Glioma.....	10
<i>Oxygen-17 ISMRM-abstracts (2020)</i>	11
Mapping neuronal activity associated with finger tapping using direct measurement of ¹⁷ O at 7 Tesla: proof-of-concept experiment.....	11
A Dedicated ¹⁷ O Rx Array to Assess Renal Metabolism of Donor Kidneys	15
<i>ISMRM Workshop-abstract (2022)</i>	19
Comparison of relative H ₂ ¹⁷ O signal in different brain lobes using dynamic ¹⁷ O MRI at 7 Tesla.....	19
<i>Our ISMRM booth wall</i>	21
Information about our booth wall.....	21
<i>Oxygen-17 ISMRM abstracts & bibliography</i>	22
<i>Our cooperation partner - Polarean</i>	23
<i>Our ISMRM rubber duck family</i>	24

Company Information



NUKEM Isotopes GmbH based in Alzenau, Germany, is a global leader in providing enriched isotopes in the form of ultra-pure substances for industry, agriculture and medical applications. We have been a reliable partner for long term demands of stable isotopes for more than two decades. We maintain our partnership with the major enrichment enterprises in Europe, the Peoples Republic of China and the Republic of Georgia. With our warehouses at Frankfurt Airport, Hamburg seaport and cooperation partners in the USA, we are able to ship our isotopes within 48 hours to our clients worldwide. With our quality management (ISO 9001-2015, NUPIC) as well as third party analysis of our products, we guarantee our customers reliable services and high-quality isotopes.

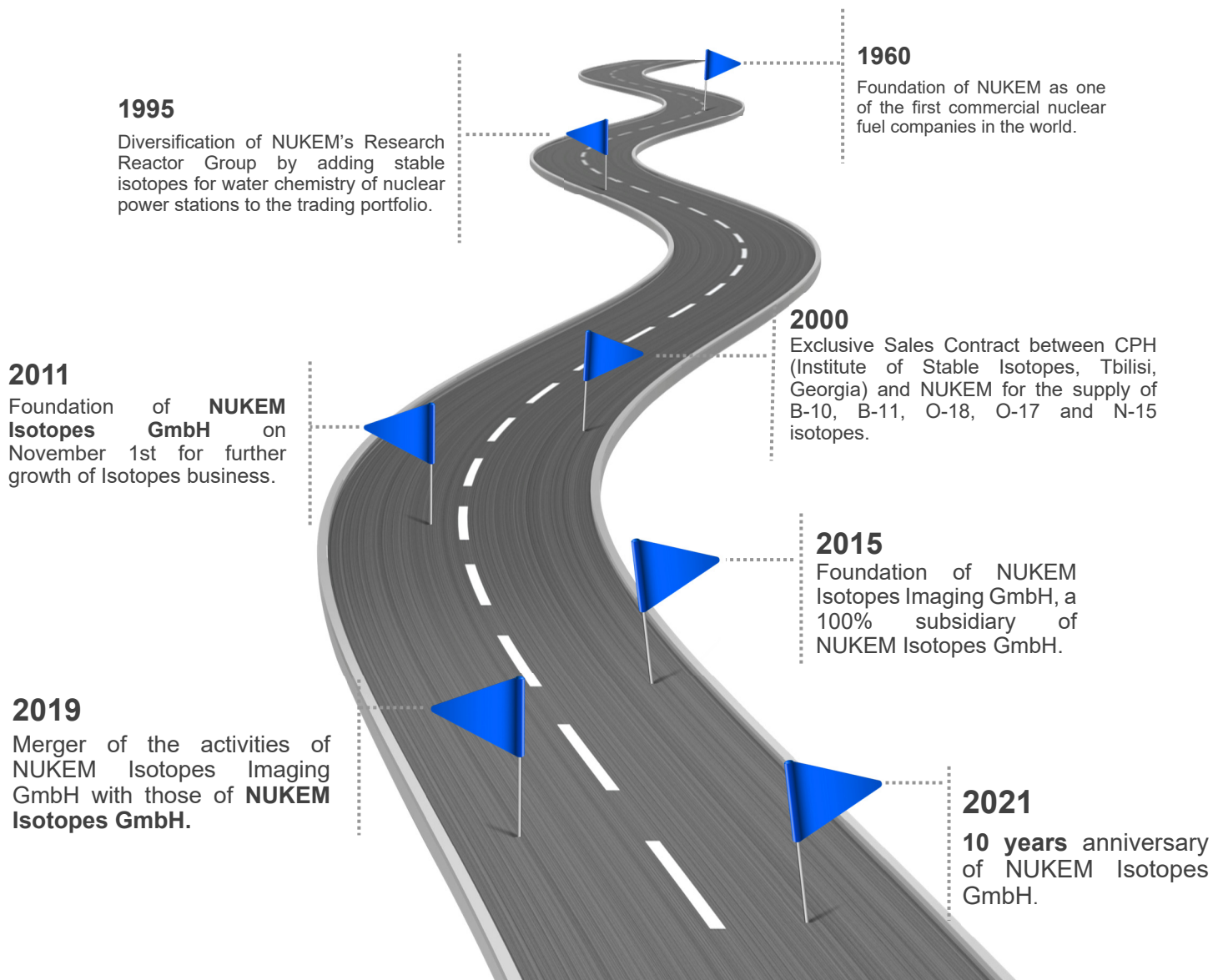
In addition, we are proud to work with major research institutes that are leaders in their field (especially in the field of MRI). Among many others, the German Cancer Research Center (DKFZ, Heidelberg), the University Hospital in Freiburg, the Research Center Juelich and the University Medical Center Groningen (UMCG) in the Netherlands should be mentioned here.

This cooperation resulted, for example, in the first $^{17}\text{O}_2$ study with 10 glioma patients, published in RSNA Radiology Journal (see page 10).

If you need more information about our company, please do not hesitate to contact us anytime at info@nukemisotopes.de.

Company History

The History of NUKEM ...



NUKEM *Isotopes* **YEARS** *Anniversary*

“We dedicate this anniversary publication to the friends of our company, our customers, suppliers, employees and retirees.”

10 years of NUKEM Isotopes

*A good reason to learn more about the history of our company and our team. Please **free download** our anniversary brochure from our homepage and find many impressions like in the picture shown below!!!*



<https://nukemisotopes.de>

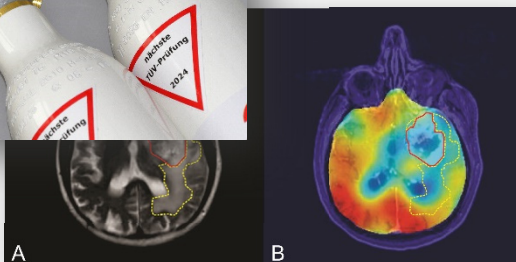
Our main imaging products



Oxygen-17

Available in the form of $^{17}\text{O}_2$, H_2^{17}O , ^{17}O -Glucose

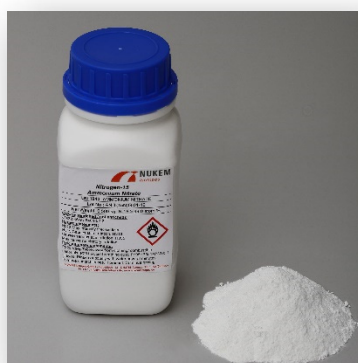
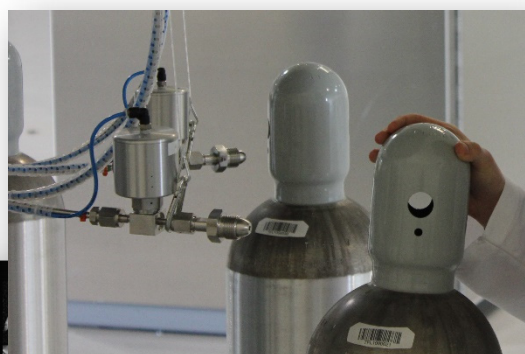
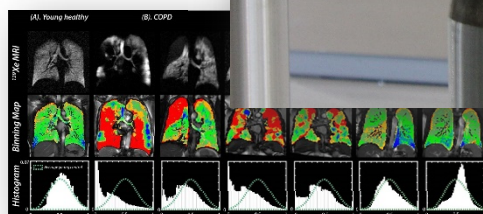
$^{17}\text{O}_2$ allows the non-invasive measurement of oxygen metabolism in tissues (mainly from the brain).



Xenon-129

Available in the form of pure Xenon

Hyperpolarized ^{129}Xe is used as non-radio-active, non-invasive MRI contrast agent for preparation of 3D lung images.



Nitrogen-15

Available in the form of $^{15}\text{N}_2$, $\text{Na}^{15}\text{NO}_3$, K^{15}NO_3 , $^{15}\text{NH}_4\text{Cl}$, $^{15}\text{NH}_4^{15}\text{NO}_3$, $(^{15}\text{NH}_4)_2\text{SO}_4$

N-15 is used in agricultural research, hyperpolarized spectroscopic imaging and in many NMR research fields more.



Oxygen-17 product information

Oxygen-17 in the form of Oxygen gas

The developments with O-17 in the form of O₂ gas in the recent years could clearly show the big advantages of the O-17 application. The enhance in quality of information about living tissue can improve the practice of medicine in the fields of cardiology, neurology and many other fields.

The magnetic properties of O-17 make it a promising “tool” for assessment of in vivo metabolic tissue information at high fields ($\geq 3T$).

If you are interested in our **¹⁷O-labeled molecules**, please do not hesitate to contact us. In cooperation with our synthesis partners, we will be able to provide you with a tailor-made offer.

The latest research results, performed with our 70at% enriched ¹⁷O₂ gas can be found on the following pages (p. 10 - 20).

Oxygen-17 Gas specification

Purity $\geq 99.9\%$

Enrichment $\geq 70\text{at}\%$

Impurities

CO ≤ 10 ppm

CO₂ ≤ 100 ppm

H₂ ≤ 50 ppm

N₂ ≤ 500 ppm

Packing

Volumes of **1 L and 2 L** are filled in Seamless stainless-steel cylinder with **50ml water volume** and a **1/4" NPT valve**



Volumes of **5 L, 10 L and 20 L** are filled in Aluminum cylinder with **400 ml water volume** and a **CGA 540 valve**



Our Oxygen-17 products are manufactured in accordance with cGMP regulations and with the requirements of 21 Code of Federal Regulations: PARTS 210 and 211.

Oxygen-17 product information

Oxygen-17 in the form of water

Oxygen-17 (^{17}O) in the form of water can be used in many fields of research. One example is the use as an MRI contrast agent for analysis of the brain cerebrospinal fluid (CSF). In addition, H_2^{17}O is the perfect precursor for the synthesis of NMR active molecules.

Oxygen-17 water specification

Purity	$\geq 99.9\%$	pH	6-8
Enrichments	10at%, 20at%, 40at%, 50at%, 60at%, 70at%, 90 at%		

Impurities*

Al	$\leq 0,05 \text{ ppm}$	Na	$\leq 1 \text{ ppm}$
Br	$\leq 0,5 \text{ ppm}$	Ni	$\leq 0,01 \text{ ppm}$
Ca	$\leq 0,1 \text{ ppm}$	NO_2	$\leq 0,1 \text{ ppm}$
Cl	$\leq 0,5 \text{ ppm}$	NO_3	$\leq 0,05 \text{ ppm}$
Co, Cr, Cu	$\leq 0,01 \text{ ppm}$	Si	$\leq 1 \text{ ppm}$
F	$\leq 0,05 \text{ ppm}$	SO_4	$\leq 0,1 \text{ ppm}$
Fe	$\leq 0,01 \text{ ppm}$	Pb	$\leq 0,01 \text{ ppm}$
K	$\leq 0,1 \text{ ppm}$	PO_4	$\leq 0,05 \text{ ppm}$
Mg	$\leq 0,05 \text{ ppm}$	Zn	$\leq 0,05 \text{ ppm}$
Mn	$\leq 0,01 \text{ ppm}$		

** applicable for 10at% enriched and 20at% enriched ^{17}O water only!*

Packing

Depending on the enrichment, we have various volumes available: **1 ml, 2 ml, 5 ml, 10 ml, 20 ml, 50ml**



Our Oxygen-17 products are manufactured in accordance with cGMP regulations and with the requirements of 21 Code of Federal Regulations: PARTS 210 and 211.

Oxygen-17 product information

Oxygen-17 in the form of D-Glucose

We are the first company in the world to synthesize substantial and high enriched amounts of single and double labelled Oxygen-17 D-Glucose. In cooperation with different research institutes, we performed the first in vivo tests with Oxygen-17 labeled D-Glucose. The results of the first experiments with Oxygen-17 labeled Glucose can be found in our ISMRM Newsletter from the last years (please visit our website - www.nukemisotopes.de - for free download of the 2017 – 2019 editions).

Oxygen-17 D-Glucose specification

Purity $\geq 95\%$

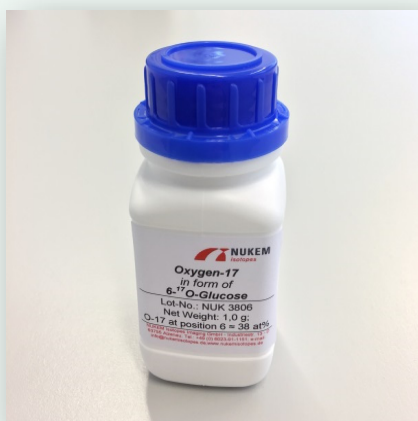
Enrichments (available on stock)

- (1) $^{17}\text{O} \geq 35\text{at\%}$ at position 6, only
- (2) $^{17}\text{O} \geq 65\text{at\%}$ at position 1, only
- (3) Double labeled Glucose: $^{17}\text{O} \geq 35\text{at\%}$ at position 6 and $^{17}\text{O} \geq 65\text{at\%}$ at position 1

We are also able to synthesize higher enrichments! Please contact us for further information.

Packing

PE- bottle with various sizes



If you are interested in other enrichments (also labelled at other positions of the glucose) or interested in other molecules, labelled with Oxygen-17, please do not hesitate to contact us.

Xenon-129 product information

Xenon-129 in the form of pure gas

Xenon-129 (Xe-129) in the hyperpolarized state is a revolutionary novel MRI contrast agent for diagnostically purposes. Xe-129 facilitates the taking of high-resolution 3D lung images by using a conventional MRI scanner.

Due to the varying solubility of Xenon in different environments, it is additionally possible to illuminate organ functions and tissue characteristics.

Our cooperation partner Polarean Imaging plc. designs and manufactures equipment for production of hyperpolarized Xenon-129. Further information about Polarean can be found in this Newsletter (see page 23).

Xenon-129 specification

Purity	$\geq 99.9\%$ for pure gas
Enrichment	$^{129}\text{Xe} \geq 80\text{at}\%$

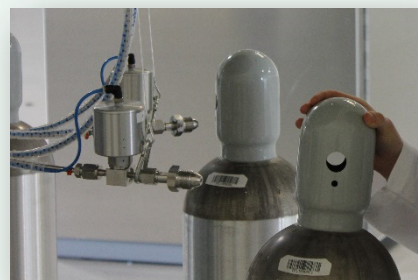
Impurities

CO	$\leq 10 \text{ ppm (pure gas)}$
CO ₂	$\leq 10 \text{ ppm (pure gas)}$
H ₂ O	$\leq 10 \text{ ppm (pure gas)}$
O ₂	$\leq 10 \text{ ppm (pure gas)}$
THC (CH ₄)	$\leq 1 \text{ ppm (pure gas)}$
TFC (CF ₄)	$\leq 5 \text{ ppm (pure gas)}$

Packing

Xenon-129 (80at%) 1,000 liter gas cylinder (with CGA 580 valve)

For other gas quantities, please [contact us \(info@nukemisotopes.de\)](mailto:info@nukemisotopes.de)



Nitrogen-15 & Oxygen-18

Nitrogen-15 in the form of gas and salts for medical and agricultural applications

Nitrogen-15 (^{15}N) is mainly used for the synthesis of ^{15}N -labelled chemical compounds. These ^{15}N -labelled compounds are used for medical and biomedical applications as well as improving the harvest in agriculture.

In recent years, great progress has also been made in the hyperpolarization of small ^{15}N -labelled molecules, which can open up many new areas of research.

Nitrogen-15 specification

Purity	$\geq 99.9\%$
Enrichment	$^{15}\text{N} \geq 99\text{at}\%$

Available compounds

Gas

Nitrogen Gas

Salts

Ammonium Chloride, Ammonium Sulphate, Potassium Nitrate, Ammonium Nitrate, Sodium Nitrate



Packing

Volume (gas)	Available in various volumes (please contact us).
Packing (salts)	400 g and/or 500 g bottles

Oxygen-18 in the form of water for medical applications

Oxygen-18 is used to synthesize radiopharmaceuticals labelled with Fluorine-18 (for example 2-fluoro-2-deoxy glucose [^{18}FDG]). These are used for Positron Emission Tomography (PET), the most common cancer diagnostic technique.

Our Oxygen-18 is available in the form of water

Purity	$\geq 99.9\%$
Enrichment	$^{18}\text{O} \geq 98\text{at}\%$, $^{17}\text{O} \leq 2\text{at}\%$, $^{16}\text{O} \leq 2\text{at}\%$
Volume	25 g & 50 g vials
Pyrogenicity	$\leq 0.25 \text{ EU/ml}$
Conductivity	$\leq 2 \mu\text{S/cm}$
pH	6 – 8



Our Oxygen-18 products are manufactured in accordance with cGMP regulations and with the requirements of 21 Code of Federal Regulations: PARTS 210 and 211.

Quantitative Dynamic Oxygen-17 MRI at 7.0 T for the Cerebral Oxygen Metabolism in Glioma

Daniel Paech, Armin M. Nagel, Miriam N. Schultheiss, Reiner Umathum, Sebastian Regnery, Moritz Scherer, Antje Wick, Tanja Platt, Wolfgang Wick, Martin Bendszus, Andreas Unterberg, Heinz-Peter Schlemmer, Mark E. Ladd, Sebastian C. Niesporek S

From the Division of Radiology, German Cancer Research Center (DKFZ), Im Neuenheimer Feld 280, 69120 Heidelberg, Germany
Published Online: Feb 18 2020; <https://doi.org/10.1148/radiol.2020191711>

ABSTRACT

Oxygen-17 MRI at 7.0 T showed that oxidative glycolysis was reduced in participants with glioma in accordance with the Warburg effect (increased glycolysis in malignancy followed by lactic acid fermentation despite abundant oxygen).

BACKGROUND

Altered metabolism is a characteristic of cancer. Because of a shift in glucose metabolism from oxidative phosphorylation to lactate production for energy generation, malignant tumors are characterized by increased glycolysis followed by lactic acid fermentation, even in the presence of abundant oxygen (the Warburg effect).

PURPOSE

To quantitatively investigate dynamic oxygen-17 (^{17}O) MRI in healthy participants and participants with untreated glioma to understand altered cerebral oxygen metabolism in glioma.

MATERIALS AND METHODS

In this prospective study conducted from September 2016 to June 2018, individuals with newly diagnosed previously untreated glioma (World Health Organization grade II–IV) and healthy volunteers were included. Dynamic ^{17}O MRI was performed with a 7.0-T whole-body system. $^{17}\text{O}_2$ gas inhalation enabled dynamic measurement of the cerebral metabolic rate of oxygen (CMRO_2) consumption. In healthy volunteers and participants with glioma, CMRO_2 values in gray matter and white matter volumes were compared by using Wilcoxon signed rank tests. In participants with glioma, the tumor volume and tumor subcompartments were compared with normal-appearing gray matter and white matter by using Friedman test followed by Holm-Sidak post hoc tests.

RESULTS

Ten participants (mean age, 42 years \pm 18 [standard deviation]; nine men) with glioma and three healthy volunteers (mean age, 44 years \pm 21; all men) were evaluated. CMRO_2 was higher in normal-appearing gray matter compared with white matter in both participants with glioma (2.36 $\mu\text{mol/g/min} \pm 0.22$ vs 0.75 $\mu\text{mol/g/min} \pm 0.10$, respectively) and healthy volunteers (2.38 $\mu\text{mol/g/min} \pm 0.15$ vs 0.63 $\mu\text{mol/g/min} \pm 0.05$, respectively) ($P < .001$ and $P = .03$, respectively). In the tumor region, CMRO_2 was reduced (high-grade tumor CMRO_2 , 0.23 $\mu\text{mol/g/min} \pm 0.07$; low-grade tumor CMRO_2 , 0.39 $\mu\text{mol/g/min} \pm 0.16$; overall CMRO_2 , 0.34 $\mu\text{mol/g/min} \pm 0.16$) compared with normal-appearing gray matter ($P < .001$) and normal-appearing white matter ($P < .001$) in accordance with the Warburg theorem.

CONCLUSION

Dynamic oxygen-17 MRI method at 7.0 T as a direct metabolic imaging technique in glioma enabled quantitative visualization of the Warburg effect. A general reduction in oxidative glycolysis was observed in accordance with the Warburg theorem.

➔ [Link: https://pubs.rsna.org/doi/10.1148/radiol.2020191711](https://pubs.rsna.org/doi/10.1148/radiol.2020191711)



Oxygen-17 ISMRM-abstracts (2020)

Mapping neuronal activity associated with finger tapping using direct measurement of ^{17}O at 7 Tesla: proof-of-concept experiment

Tanja Platt¹, Louise Ebersberger^{2,3}, Vanessa L Franke^{1,4}, Armin M Nagel^{1,5,6}, Reiner Umathum¹, Heinz-Peter Schlemmer², Peter Bachert^{1,4}, Mark E Ladd^{1,3,4}, Andreas Korzowski¹, Sebastian C Niesporek¹, and Daniel Paech²

¹Medical Physics in Radiology, German Cancer Research Center, Heidelberg, Germany, ²Radiology, German Cancer Research Center, Heidelberg, Germany, ³Faculty of Medicine, University of Heidelberg, Heidelberg, Germany, ⁴Faculty of Physics and Astronomy, University of Heidelberg, Heidelberg, Germany, ⁵Institute of Radiology, University Hospital Erlangen, Erlangen, Germany, ⁶Institute of Medical Physics, Friedrich-Alexander-Universität Erlangen-Nürnberg (FAU), Erlangen, Germany

SYNOPSIS Dynamic ^{17}O -MRI enables direct quantification of the cerebral metabolic rate of oxygen (CMRO_2) consumption. We investigated hemispherical dependence of the method in three healthy volunteers as well as its potential for mapping neuronal activity associated with finger tapping in one healthy volunteer. Our findings were consistent with previous results, demonstrating higher CMRO_2 values in gray compared to white matter. Evaluation of left/right hemispheric CMRO_2 values without sensorimotor stimulation demonstrated hemispherical independence of the technique. The finger-tapping experiment demonstrated increased ^{17}O -signal in the stimulated sensorimotor cortex and adjacent brain tissue, indicating that dynamic ^{17}O -MRI may permit visualization of physiological neuronal activity.

PURPOSE Dynamic ^{17}O -MRI enables metabolic imaging with reproducible quantification of the cerebral metabolic rate of oxygen (CMRO_2) consumption in healthy volunteers ¹ and patients with glioma ². This imaging technique requires inhalation of enriched $^{17}\text{O}_2$ gas. Data of three healthy volunteers were investigated with regard to hemispherical dependence of CMRO_2 quantification and robustness of the method. Mapping of task-related neuronal activity was investigated in one healthy volunteer employing finger tapping and dynamic ^{17}O -MRI.

METHODS All experiments were performed on a 7-T whole-body MR system (Siemens, Erlangen, Germany). For the investigation of hemispherical dependence, three healthy volunteers (44 ± 21 years, all men) were included in this study ($n=3$, 6 datasets). A home-built double-resonant $^{17}\text{O}/^1\text{H}$ head coil was used to acquire dynamic ^{17}O data as well as basic proton images. A 24-channel ^1H head coil (Nova Medical, Wilmington, Massachusetts) was used to obtain high spatial resolution anatomical data. Oxygen MRI data were acquired with a density-adapted radial sequence ³ with a Golden Angle distribution of projections ⁴ (nominal spatial resolution of $(7.5\text{mm})^3$, $\text{TR}/\text{TE}=20\text{ms}/0.56\text{ms}$, acquisition time $t=40\text{min}$). Administration of ca. 4.0L of 70%-enriched $^{17}\text{O}_2$ gas enabled the determination of the cerebral metabolic rate of oxygen (CMRO_2) consumption via three-phase inhalation experiment (baseline phase, $^{17}\text{O}_2$ inhalation phase, decay phase) ^{1,5}. The segmentation masks for gray matter (GM) and white matter (WM) were created automatically using the FSL-FAST algorithm tool ⁶ and were used for partial volume correction ⁷. All segmentation masks were subdivided into two compartments (left and right hemisphere) to investigate possible hemispherical dependence of CMRO_2 values. The CMRO_2 values for gray and white matter as well as their hemispherical dependence (left versus right hemisphere) were tested using Wilcoxon signed-rank tests with a level of significance of $p < 0.05$. The experiment for mapping neuronal activity included dynamic ^{17}O -MRI in one healthy volunteer (68 years, male). A finger-tapping paradigm was employed for stimulating the sensorimotor cortex. The chosen paradigm alternated blocks of resting and sequential right-hand finger-to-thumb tapping. A total of 40 images were acquired in 40 blocks of 60 seconds with the same experimental setup as for investigation of regional dependence.

Oxygen-17 ISMRM-abstracts (2020)

RESULTS Dynamic ^{17}O -signals relative to the baseline show similar increases in the left and right brain hemispheres (LH, RH) for both gray matter and white matter (Fig. 1A). Increased CMRO_2 in gray matter ($2.38 \pm 0.15 \mu\text{mol/g/min}$) was observed compared to white matter ($0.63 \pm 0.05 \mu\text{mol/g/min}$) ($p=0.03$) (Fig. 1B). Furthermore, the obtained CMRO_2 values in gray matter and white matter are consistent with previous studies in healthy volunteers (gray matter: $1.42\text{--}3.57 \mu\text{mol/g/min}$, white matter: $0.67\text{--}0.75 \mu\text{mol/g/min}$) ^{1,5,8}. The comparison between left and right hemispheric CMRO_2 in gray and white matter did not show any significant differences ($p=0.50$ and $p=0.25$) (Fig. 1B). The neuronal activity experiment with the finger-tapping paradigm (right-hand tapping) employing dynamic ^{17}O -MRI yielded higher ^{17}O -signal increases in the left sensorimotor cortex and adjacent brain tissue compared to the contralateral brain region as well as the experiment without finger tapping (Fig. 2).

DISCUSSION Dynamic ^{17}O -MRI represents a non-invasive method to specifically quantify oxygen-dependent energy metabolism. Our findings for ^{17}O -MRI of three healthy volunteers without sensorimotoric stimulation showed that CMRO_2 was higher in gray matter compared to white matter, without significant differences between the left and right hemisphere. This indicates hemispherical independence of the employed dynamic ^{17}O -MRI technique. The high increase in ^{17}O -signal in brain regions related to sensorimotoric stimulation during finger tapping suggests that dynamic ^{17}O -MRI may enable visualization of task-related neuronal activity in the healthy human brain. This finding is in agreement with a previous study in which mapping of neuronal activity was shown to be feasible using visual stimulation ⁹.

CONCLUSION Dynamic ^{17}O -MRI demonstrates potential as a robust and non-invasive MRI technique that enables direct metabolic imaging in humans. The finger-tapping experiment in one healthy volunteer showed increased ^{17}O -signal in the stimulated brain region. Therefore, dynamic ^{17}O -MRI may permit visualization of physiological neuronal activity.

ACKNOWLEDGEMENTS

The authors would like to thank NUKEM Isotopes GmbH for their supply of $^{17}\text{O}_2$ gas and support of this project.

REFERENCES

1. Niesporek, SC, et al. Magn Reson Med 2018; 79: 2923–2934;
2. Niesporek SC, et al. In Proc. ISMRM 2018; #625;
3. Nagel, AM, et al. Magn Reson Med 2009; 62: 1565-1573;
4. Chan, RW, et al. Magn Reson Med 2009; 61(2): 354-63
5. Atkinson IC and Thulborn KR. Neuroimage 2010; 51: 723-33;
6. Zhang, Y, et al. IEEE Trans Med Imaging 2001; 20: 45-57;
7. Niesporek, SC, et al. Neuroimage 2015;112: 353-363;
8. Hoffmann SH, et al. MAGMA 2014; 27: 579-87;
9. Zhu, X, et al. In Proc. ISMRM 2006; #409;

SESSION Biophysics & Metabolism Studied with Imaging & Spectroscopy of Non-Hyperpolarized X-Nuclei

Day/Date: Wednesday, 22 April 2020

Session Time: 08:15“

FIGURES

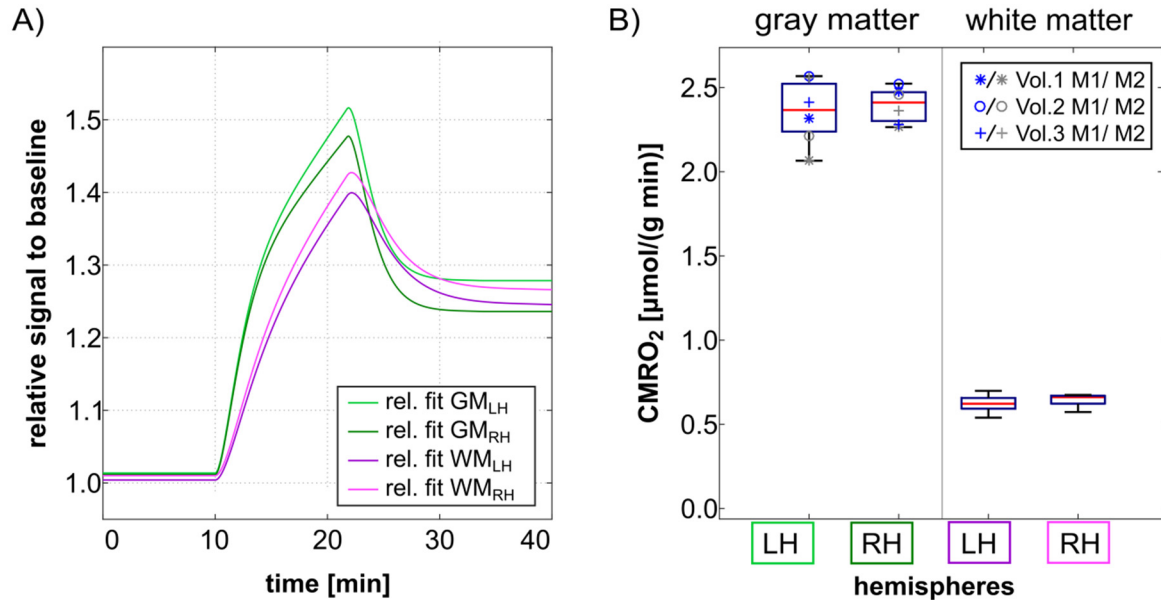


Fig. 1: A) Dynamic ^{17}O -signal curve relative to the baseline shows similar increases for gray matter (GM) in the left and right brain hemispheres (LH, RH) and also for white matter (WM). B) CMRO₂ values for GM and WM in LH and RH of three healthy volunteers (Vol.1-3, 28-65 y.o., for two different measurements (M1, M2)). Increased CMRO₂ in gray matter was observed compared to white matter ($p=0.03$). The comparison between LH and RH CMRO₂ does not show any significant differences in gray matter, nor in white matter ($p=0.50$ and $p=0.25$, respectively).

Oxygen-17 ISMRM-abstracts (2020)

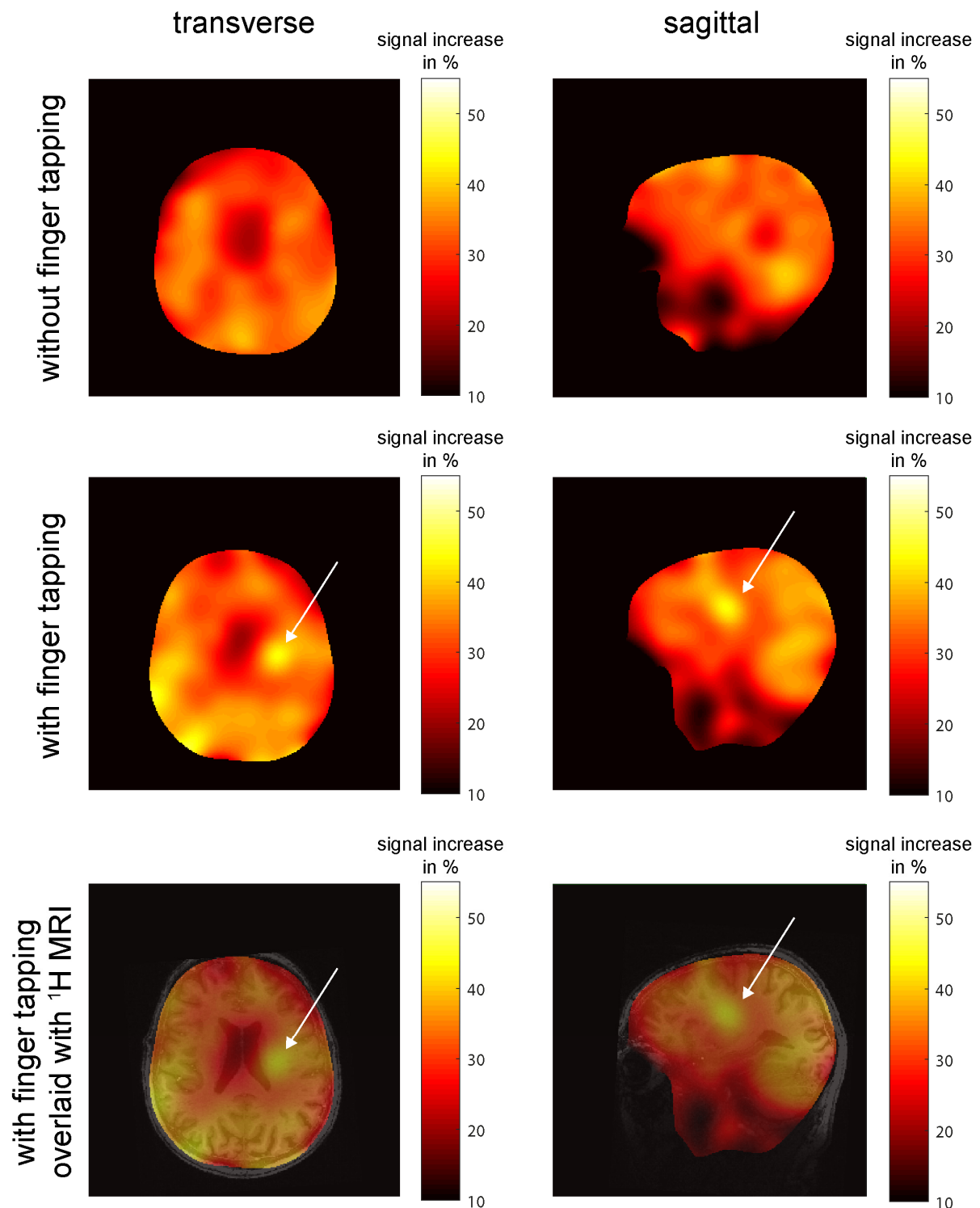


Fig. 2: ^{17}O -signal increase between the beginning of the inhalation phase and the end of the inhalation phase (in %). The map without stimulation by finger tapping shows uniform distribution of signal increase; for the experiment with stimulation there is a high signal increase in brain regions related to sensomotoric stimulation. In the bottom row, the map with finger tapping is overlaid with an anatomical MPRAGE image.

A Dedicated ^{17}O Rx Array to Assess Renal Metabolism of Donor Kidneys

Ali Caglar Özen^{1,2}, Johannes Fischer¹, Hao Song¹, Yanis Taege¹, Christian Schuch³, Rianne Schutter⁴, Cyril Moers⁴, Ronald JH Borra⁵, Michael Bock¹

¹Dept. of Radiology, Medical Physics, Medical Center – University of Freiburg, Faculty of Medicine, University of Freiburg, Freiburg, Germany, ²German Consortium for Translational Cancer Research Partner Site Freiburg, German Cancer Research Center (DKFZ), Heidelberg, Germany, ³NUKEM Isotopes GmbH, Alzenau, Germany ⁴Department of Surgery – Organ Donation and Transplantation, University Medical Center Groningen, Groningen, Netherlands, ⁵Medical Imaging Center, University Medical Center Groningen, Groningen, Netherlands

SYNOPSIS Direct ^{17}O -MRI can be used to measure renal metabolism in perfused kidneys in an organ transplantation setup. To optimize SNR, a dedicated ^{17}O Rx array was designed that fits into a perfusion box used for functional metabolism tests of the donor kidneys. The increased filling ratio resulted in higher SNR compared to the volume and surface Tx/Rx coils. In combination with a ^{17}O birdcage Tx coil for homogeneous excitation the 4-element Rx array could also be used for parallel imaging.

INTRODUCTION Most organ transplants are renal transplants [1–3], but even though biomarkers exist to diagnose complications after kidney transplantation [4], survival rates decrease drastically with the time after transplantation [5,6]. One reason for post-transplantation complications is the insufficient functional characterization of the transplanted kidney. We have shown previously that, in addition to perfusion and renal filtration, tissue oxygenation of a resected kidney can be quantified in vitro before implantation using dynamic ^{17}O MRI [7].

A homogeneous excitation field (B1) and high SNR are important for high-resolution ^{17}O MRI of the kidney, which in whole body ^1H MRI is achieved by combining a local Rx array with a large volume Tx coil. In this work, we designed and constructed a ^{17}O RF coil array that fits on a sterilized perfusion box used for functional metabolism tests of the donor kidneys which was combined with a ^{17}O birdcage head coil for homogeneous RF excitation.

METHODS Rx Array A schematic of the coil arrangement is shown in Figure 1A. Three of the 4 Rx elements (C1-C3) were mounted on a 3D-printed holder (Fig.1B) that fits under the perfusion box in which the kidney is stored between resection and transplantation. C1-C3 were constructed using two turns of a tin-plated copper wire ($\phi=1\text{mm}$) on a rectangular shaped former of $3\times 5\text{cm}^2$ size. The tuning capacity was distributed on two elements, one of which was used as the input port for tuning and matching (Fig.1C). A larger ($\phi=15\text{cm}$) Rx element (C4) was placed on top of the perfusion box using a single turn ($\phi=5\text{mm}$) of copper tube (Fig.1D). C2-4 were geometrically decoupled, and all elements were further isolated from each other by preamplifier decoupling [8]. A separate custom-made quadrature-driven 4-leg birdcage volume coil was used as the Tx only element. Measurement of the reflection and transmission coefficients, S_{ij} , were performed on a vector network analyzer (ZVB 4; Rohde&Schwarz, Munich Germany) for each channel pair with all other channels terminated with 50Ω . Noise correlation matrix of the Rx array was also measured using a FID sequence (TR/TE 200 ms/0.56 ms, BW 10 kHz, Peak Tx RF voltage 0V) [9].

MRI Measurements A cylindrical water phantom composed of three separate compartments was used to test performance of the coil array at a clinical 3T MR system (Prisma; SIEMENS, Erlangen, Germany). The inner cylinder (modeling the medulla) was filled with $^{17}\text{O}_2$ -enriched saline solution ($c_{^{17}\text{O}_2} = 0.072\%$) and has an inner diameter of 3 cm and a length of 4 cm. In total, volume ($V = 247\text{mL}$) and axial dimensions are similar to those of a human kidney [10]. For image acquisition a radial 3D UTE sequence with golden-angle projection acquisition pattern was used [11]. Kaiser-Bessel-regridding [12] of k-space data and Hanning-filtering was subsequently applied. For comparison, a custom built Tx/Rx head coil, and a loop coil were also used to acquire ^{17}O MRI data using the same protocol (TR/TE 6ms/0.52ms, FA $\pi/6$, BW 390 Hz/px, radial spokes 80000). The SNR of a measurement was quantified according to [13].

Oxygen-17 ISMRM-abstracts (2020)

RESULTS S-parameter and noise correlation matrices are shown Figure 2. The range of coupling between overlapping/non neighboring elements was 13.5-21.3 dB/ 13.5-18.3 dB, to which preamplifier decoupling (75cm-long coaxial line and lumped element 3l/16 tank circuits between coil and preamplifier interface) added another 13 dB. An average unloaded/loaded quality factor of $Q_U = 150.3 / Q_L = 80.2$ was measured resulting in a Q-ratio of 1.87. The active detuning efficiency was measured as 38+-3 dB for all elements. Noise correlation values ranged from 4% to 10% (Fig.2). The reconstructed images of the kidney phantom are shown in Figure 3 as cross-sections from different axes. The SNR values of the center/left/right section of the phantom are 98/66/81 for single loop coil, 97/65/70 for the birdcage coil, and 481/425/404 for the ^{17}O Rx array, respectively, which is an up to 5-fold increase in SNR using the Rx array.

DISCUSSION As expected, the SNR of the central cylinder was higher for all coils due to the addition of H_2^{17}O . The performance of the Rx array was superior to single channel Tx/Rx loop and birdcage coils due to the smaller coil element size, and the higher filling ratio. Single loop coils, however, are not preferable for quantitative imaging tasks due to an SNR difference of 19% between left and right cylinders, in the SNR comparison. C4 is placed on top of the perfusion box, therefore has higher coupling with C1-3. Since there is a distance of at least 8 cm between the center of the kidney and the loop coil, fields of a smaller loop coil would not be able to penetrate deep enough to reach the kidney. In a next step the increased image quality of the coil array will be used to increase the spatial and temporal resolution in dynamic ^{17}O MRI measurements in kidneys to identify e.g. induced ischemic lesions.

ACKNOWLEDGEMENTS Support from NUKEM Isotopes Imaging GmbH is gratefully acknowledged.

REFERENCES

1. Branger, P. & Samuel, U. Annual Report 2017. 124 (Eurotransplant International Foundation, 2017).
2. Hart, A. et al. OPTN/SRTR 2016 Annual Data Report: Kidney. Am. J. Transplant. 18, 97.
3. Department of Health and Human Services, Health Resources and Services Administration, Healthcare Systems Bureau, Division of Transplantation. Annual Report of the U.S. Organ Procurement and Transplantation Network and the Scientific Registry of Transplant Recipients: UNOS (2016). Available at: <https://unos.org/about/annual-report/2016-annual-report/>. (Accessed: 30th October 2018).
4. Salvadori, M. & Tsalouchos, A. Biomarkers in renal transplantation: An updated review. World J. Transplant. 7, 161–178 (2017).
5. Pestana, J. M. Clinical outcomes of 11,436 kidney transplants performed in a single center - Hospital do Rim. J. Bras. Nefrol. 39, (2017).
6. Wang, J. H., Skeans, M. A. & Israni, A. K. Current Status of Kidney Transplant Outcomes: Dying to Survive. Adv. Chronic Kidney Dis. 23, 281–286 (2016).
7. Taege, Y., Fischer, J., Özen, A. C., et al. Protocol Optimization for Functional ^{17}O -MRI of Donor Kidneys at 3T. In Proc. 27th ISMRM, Montreal, QC, Canada. p. 4223.
8. Roemer, P.B., Edelstein, W.A., Hayes, C.E., Souza, S.P., Mueller, O.M. The NMR phased array, Magnetic Resonance in Medicine 16, 192–225 (1990).
9. Kellman, P., & McVeigh, E. R. Image reconstruction in SNR units: a general method for SNR measurement. Magnetic resonance in medicine, 54(6), 1439–1447 (2005).
10. Cheong, B. et al. Normal values for renal length and volume as measured by magneticresonance imaging. Clinical Journal of the American Society of Nephrology 2.1 (2007).

Oxygen-17 ISMRM-abstracts (2020)

11. Chan, R. W., Ramsay, E. A., Cunningham, C. H. & Plewes, D. B. Temporal stability of adaptive 3D radial MRI using multidimensional golden means. *Magn. Reson. Med.* 61, 354–363 (2009).
12. Jackson, J. I., Meyer, C. H., Nishimura, D. G. & Macovski, A. Selection of a convolution function for Fourier inversion using gridding (computerised tomography application). *IEEE Trans. Med. Imaging* 10, 473–478 (1991).
13. Gudbjartsson, H. H. and Patz, S. The Rician Distribution of Noisy MRI Data. *Magnetic Resonance in Medicine* 34.6 (1995).

FIGURES

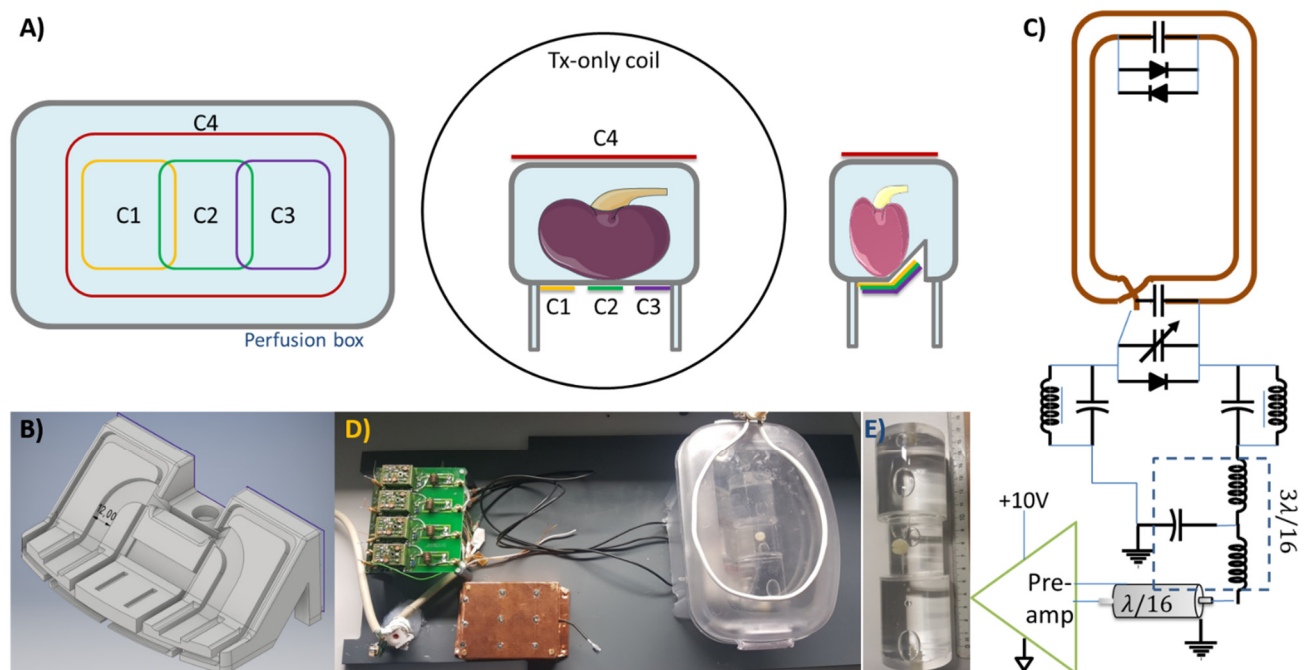


Fig.1: Kidney ^{17}O coil system.

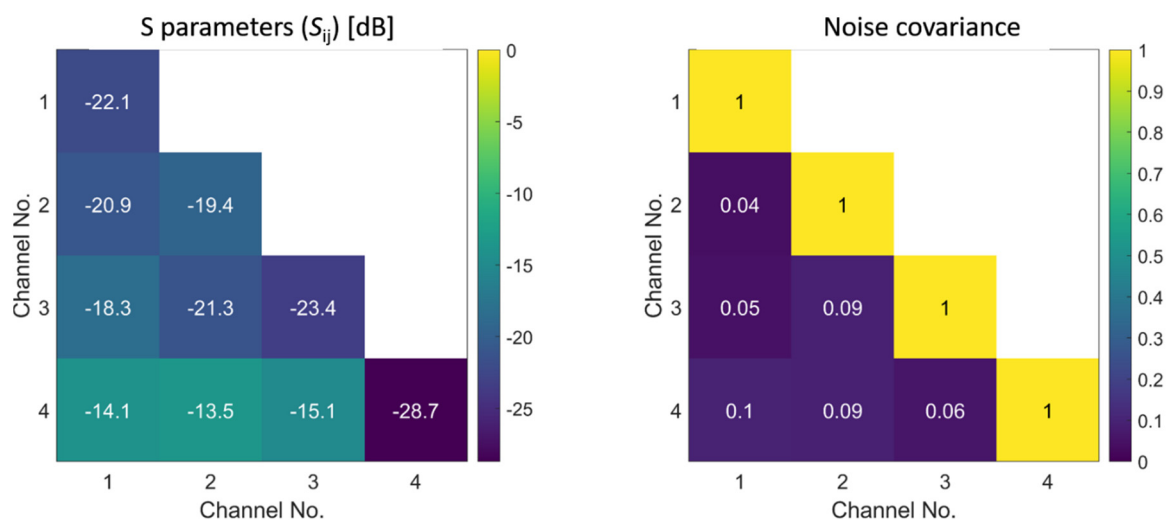


Fig.2: S parameters and decoupling matrix + noise cov.

Oxygen-17 ISMRM-abstracts (2020)

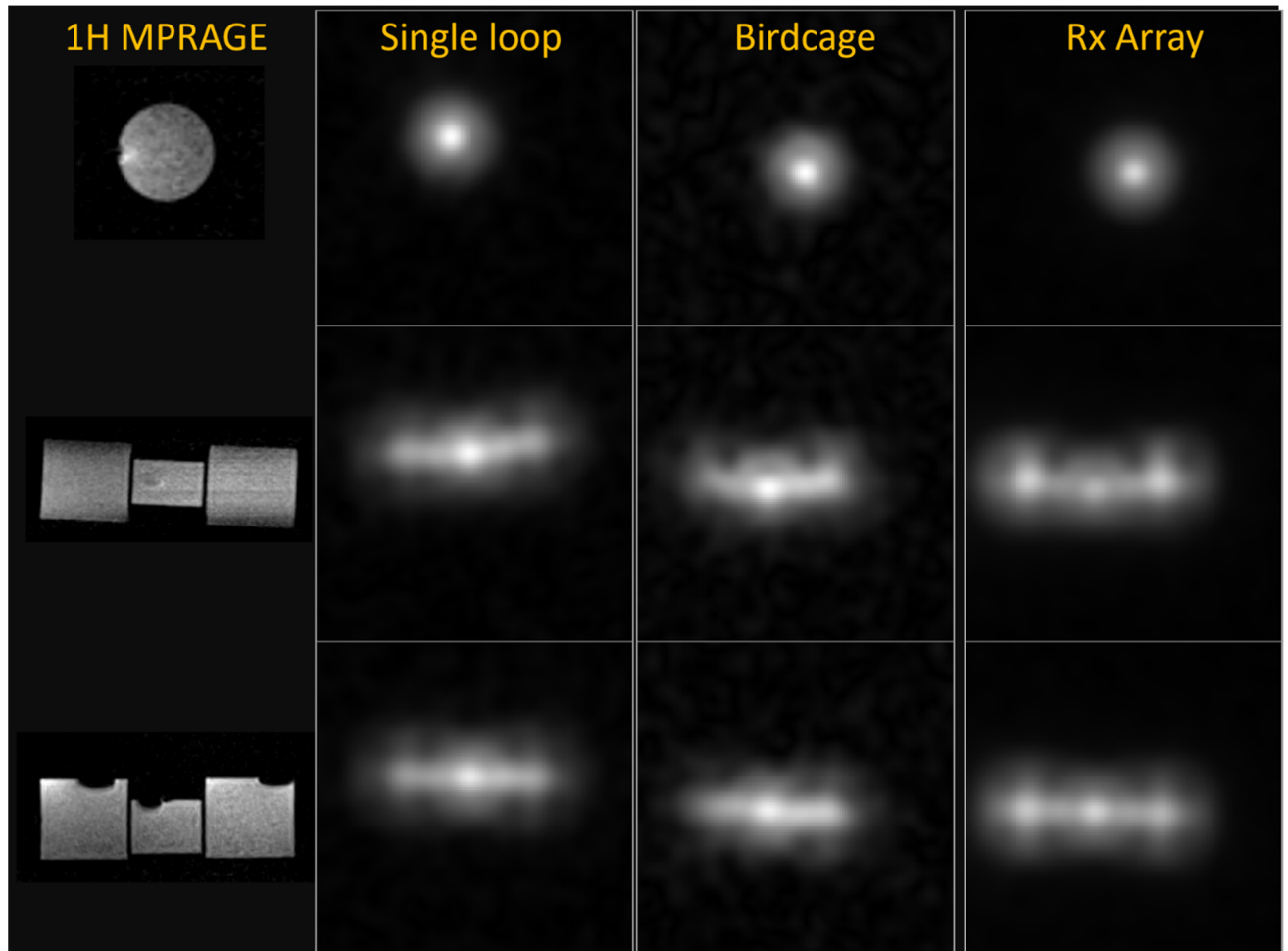


Fig.3: ^{17}O MRI images of kidney phantom with MPRAGE reference.

Presented on ISMRM Workshop on Ultra-High Field MR (19-22 March 2022) in Lisbon, Portugal

Comparison of relative $H_2^{17}O$ signal in different brain lobes using dynamic ^{17}O MRI at 7 Tesla

Louise Ebersberger^{1,2}, Fabian J. Kratzer³, Reiner Umathum³, Armin M. Nagel^{3,4}, Heinz-Peter Schlemmer¹, Mark E. Ladd^{2,3}, Daniel Paech^{1,5}, Tanja Platt³

¹ Radiology Department, German Cancer Research Center, ² Medical Faculty, University of Heidelberg, ³ Department of Medical Physics in Radiology, German Cancer Research Center, ⁴ Radiology Institute, University Hospital Erlangen, ⁵ Clinic for Neuroradiology, University Hospital Bonn

TARGET AUDIENCE The target audience of this study is interdisciplinary and includes scientists in neurophysiology interested in the cerebral oxygen metabolism, particularly neuronal activity, as well as all researchers working with ^{17}O MRI.

PURPOSE The purpose of this study was to investigate potential metabolic differences in the human brain lobes, thus adding to fundamental neurophysiological research. Secondly, this study was conducted to identify possible confounding factors when researching neuronal activity using dynamic ^{17}O MRI.

METHODS Two healthy volunteers (all men, 31 and 68 years) were included in this study. Both participants were scanned twice in a 7 Tesla whole-body MR system (Siemens, Erlangen, Germany) yielding a total of four data sets. A home-built double-resonant $^{17}O/^1H$ head coil enabled the acquisition of oxygen data and basic 1H images; the high-resolution anatomical data was obtained with a 24-channel 1H head coil (Nova Medical, Wilmington, Massachusetts). The ^{17}O data were acquired using a density-adapted radial sequence [1] with a Golden Angle distribution of projections (TR/TE=20ms/0.56ms, tAcq=40min, nominal spatial resolution=(7.5mm)³) [2]. During the three-phase experiment (baseline, inhalation phase, decay phase) [3] the participants inhaled approximately 4.0L of 70%-enriched $^{17}O_2$ gas. The experimental set-up has previously been described in detail [4]. The FSL FAST-algorithm [5] was applied for automatic segmentation into gray matter (GM) and white matter (WM). 3D-masks of the brain lobes (frontal, parietal, temporal, occipital) were created manually. Data analysis comprised the evaluation of the relative $H_2^{17}O$ signal evolution and visual comparison of the brain lobes in ^{17}O images showing the relative signal increase between baseline and end of inhalation phase.

RESULTS The evaluation of the relative signal evolution showed the highest relative $H_2^{17}O$ signal increase in the occipital lobe in all four measurements for both tissue types, GM and WM. For GM, the lowest relative $H_2^{17}O$ signal increase was found consistently in the frontal lobe in all experiments, while the results for WM did not show a clear tendency. The comparison between the other two brain lobes did not afford any trend in favor of the one or other. The relative signal evolution for GM and WM in volunteer 1 (V1), experiment 1 (exp. 1) is depicted in Fig. 1. The corresponding relative ^{17}O MRI images visually showed a higher $H_2^{17}O$ signal increase in the occipital lobe compared to the frontal, parietal and temporal lobe, as can be seen in Fig. 2.

DISCUSSION Dynamic ^{17}O MRI is a useful imaging technique for researching the brain's oxygen metabolism. The evaluation of the $H_2^{17}O$ signal dynamics in different volumes furnishes direct information about the regional oxygen turnover. In this abstract, we investigated the $H_2^{17}O$ signal within the frontal, parietal, temporal and occipital lobe, and separated in GM and WM, in four data sets. However, due to a nominal resolution of (7.5mm)³, the relative curves are affected by partial volume effects.

The evaluation of the relative signal evolution showed a trend to a higher relative $H_2^{17}O$ signal increase in the occipital lobe, for GM as well as WM, in comparison with the other three

investigated brain lobes. In contrast, the frontal lobe showed a lower relative $H_2^{17}O$ signal increase for GM in comparison to the other brain regions.

For one, this could be caused by a higher GM to WM ratio in the occipital lobe and a lower ratio in the frontal lobe. A higher oxygen metabolism in the occipital lobe might also be due to a physiologically higher brain activity in the visual cortex, located in the occipital lobe, compared to other brain areas. In context, Song et al. recently investigated the oxygen consumption in the frontal, parietal and occipital lobe of one healthy volunteer using ^{17}O MRI at 3 Tesla, also without taking partial volume effects into account [6]. Here, the oxygen consumption afforded homogenous results for WM in all three brain lobes. For GM, the parietal and frontal lobe showed higher values in oxygen turnover compared to the occipital lobe [6]. However, Ibaraki et al. found higher oxygen consumption within the occipital lobe, and the lowest oxygen turnover in the frontal lobe using 2D and 3D ^{15}O PET, when comparing the same four brain lobes as in our study [7].

Future studies including more subjects may allow a more detailed investigation of the oxygen consumption in the different lobes. The influence of partial volume effects might also be investigated in more detail in this context.

CONCLUSION The results of this study suggest a higher relative $H_2^{17}O$ signal increase within the occipital lobe compared to the frontal, parietal, and temporal lobe. This information might need to be taken into account as a possible confounding factor when investigating neuronal activity employing dynamic ^{17}O MRI using a visual stimulus paradigm.

ACKNOWLEDGEMENTS The authors thank NUKEM Isotopes GmbH for the supply of ^{17}O gas at a reduced cost.

REFERENCES

1. Nagel, A.M., et al., *Sodium MRI using a density-adapted 3D radial acquisition technique*. Magn Reson Med, 2009. **62**(6): p. 1565-73.
2. Chan, R.W., et al., *Temporal stability of adaptive 3D radial MRI using multidimensional golden means*. Magn Reson Med, 2009. **61**(2): p. 354-63.
3. Atkinson, I.C. and K.R. Thulborn, *Feasibility of mapping the tissue mass corrected bioscale of cerebral metabolic rate of oxygen consumption using 17-oxygen and 23-sodium MR imaging in a human brain at 9.4 T*. Neuroimage, 2010. **51**(2): p. 723-33.
4. Niesporek, S.C., et al., *Reproducibility of CMRO2 determination using dynamic (17) O MRI*. Magn Reson Med, 2018. **79**(6): p. 2923-2934.
5. Zhang, Y., M. Brady, and S. Smith, *Segmentation of brain MR images through a hidden Markov random field model and the expectation-maximization algorithm*. IEEE Trans Med Imaging, 2001. **20**(1): p. 45-57.
6. Song, H., et al., *Regional Analysis of CMRO2 in Human Brain Using Dynamic (17)O-MRI*. In Proc. ISMRM 2020. **#482**
7. Ibaraki, M., et al., *Quantification of cerebral blood flow and oxygen metabolism with 3-dimensional PET and 15O: validation by comparison with 2-dimensional PET*. J Nucl Med, 2008. **49**(1): p. 50-9.

FIGURES

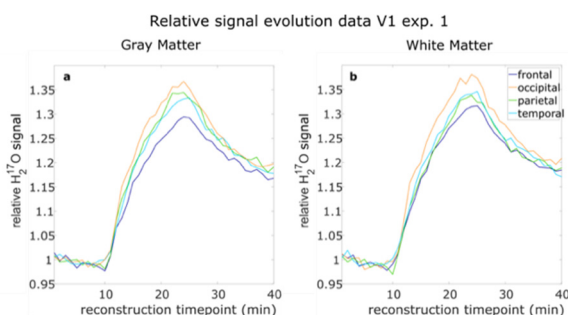


Fig. 1: Relative $H_2^{17}O$ signal evolution of V1, exp. 1 for a) GM and b) WM. The occipital lobe (orange) shows a steeper slope and a higher maximum compared to the frontal, parietal and temporal lobe. The frontal lobe (navy) afforded the lowest relative $H_2^{17}O$ maximum.

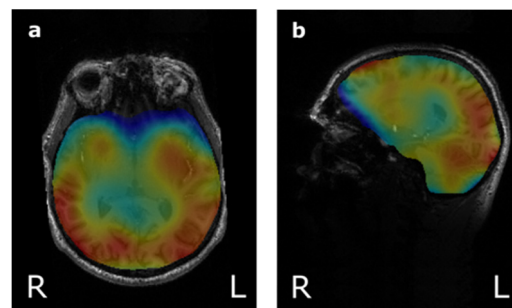


Fig. 2: ^{17}O MRI images of V1, exp. 1 showing the relative signal change due to the ^{17}O inhalation, a) transversal and b) sagittal. In this map, the occipital lobe visually shows a higher relative $H_2^{17}O$ signal compared to the other brain lobes, especially the frontal and parietal lobe (seen in b).

Our ISMRM booth wall

Your global supplier for stable isotopes

A photograph of a booth wall display for NUKEM Isotopes. The display features a central hexagonal graphic with the text "Stable Isotopes for medical application". Surrounding this central graphic are five other hexagonal graphics, each containing text and images related to a specific isotope application:

- ^{17}O Oxygen**: "is the only non-radioactive isotope to measure oxygen consumption and metabolism in real-time by using MRI systems for diagnostic applications and medical research." Includes images of MRI scans and a diagram.
- ^{129}Xe Xenon**: "in the hyperpolarized state is a revolutionary novel MRI contrast agent for diagnostic purposes. ^{129}Xe makes it possible to take high-resolution 3D lung images by using a conventional MRI scanner." Includes an image of a person in an MRI scanner.
- ^{18}O in the form of water, gas and D-Glucose**: Includes an image of vials.
- ^{129}Xe in the form of pure gas and mixtures**: Includes an image of a person in an MRI scanner.
- ^{13}C in the form of pure gas and mixtures**: Includes an image of a person in an MRI scanner.

 At the bottom of the booth wall, the text "Realizing ideas with isotopes" is displayed, followed by the website "nukem-isotopes.com".

Information about our booth wall

The $^1\text{H}/^{17}\text{O}$ -MRI images and diagrams on our wall (top, left side) were, thankfully, provided by the German Cancer Research Center (DKFZ), Heidelberg, Germany and University Hospital Erlangen, Erlangen, Germany.

The displayed images and diagrams are part of the study Quantitative Dynamic Oxygen-17 MRI at 7.0 T for the Cerebral Oxygen Metabolism in Glioma (see page 9 for further information).

In addition, the MRI lung images (on the right side) were, thankfully, provided by Duke University, Durham, NC (Bastiaan Driehuys) and the image of the Xe-129 Polarizer was gratefully provided to us by our business partner Polarean.

Oxygen-17 ISMRM abstracts & bibliography

ISMRM 2021 abstract/presentations

1. Dynamic Oxygen-17 MRI with Model-Based Approach for Mapping Cerebral Metabolic Rate of Oxygen in Mouse Brain at 9.4 T; Yuning Gu, Huiyun Gao, Kihwan Kim, Yunmei Wang, and Xin Yu 1800
2. Measuring CMRO₂ in Brain Subcortical Structures Using Dynamic ¹⁷O-MRI; Hao Song, Burak Akin, Johannes Fischer, Ali Caglar Özen, Stefan Schumann, and Michael Bock 1796
3. New tuHDC BST-BT Ceramics with Optimal Permittivity Greatly Improve B1 efficiency and SNR at Room Temperature for ¹⁷O MRSI Application at 10.5T; Hannes Michel Wiesner, Xiao-Hong Zhu, Maryam Sarkarat, Xin Li, Matt Waks, Michael T. Lanagan, Qing X. Yang, and Wei Chen 1808
4. Single Loop Tri-frequency Surface Coil Design for ¹H MRI and Interleaved Dynamic ²H and ¹⁷O MRS Applications at Ultrahigh Field of 16.4T; Parker John Bresnahan Jenkins, Guangle Zhang, Wei Zhu, Xiao-Hong Zhu, and Wei Chen 1816.

ISMRM 2020 abstract/presentations

1. Mapping neuronal activity associated with finger tapping using direct measurement of ¹⁷O at 7 Tesla: proof-of-concept experiment; Tanja Platt, Louise Ebersberger, Vanessa L Franke¹, Armin M Nagel¹, Reiner Umathum, Heinz-Peter Schlemmer, Peter Bachert, Mark E Ladd, Andreas Korzowski, Sebastian C Niesporek, and Daniel Paech 0472.
2. Direct ¹⁷O-ZTE-MRI reveals decreased cerebral metabolic rate of oxygen consumption in a murine model of amyloidosis; Celine Baligand, Jean-Baptiste Perot, Didier Thenadey, Julien Flament, Marc Dhenain, and Julien Valette 0481.
3. Regional Analysis of CMRO₂ in Human Brain Using Dynamic ¹⁷O-MRI; Hao Song, Yanis Taege, Johannes Fischer, Ali Caglar Özen, and Michael Bock 0482.
4. Dynamic Oxygen-17 MRI with Adaptive Reconstruction using Golden-Means-Based 3D Radial Sampling; Yuning Gu, Huiyun Gao, Kihwan Kim, Ciro Ramos-Estebanez, Yunmei Wang, and Xin Yu 2998.
5. A Dedicated ¹⁷O Rx Array to Assess Renal Metabolism of Donor Kidneys, Ali Caglar Özen, Johannes Fischer, Hao Song, Yanis Taege, Christian Schuch, Rianne Schutter, Cyril Moers, Ronald JH Borra, Michael Bock

ISMRM 2019 abstract/presentations

1. Sebastian Niesporek, Nina Weinfurter, Armin Nagel, Mark Ladd, Heinz-Peter Schlemmer, Daniel Paech; Metabolic Brain Tumor Analysis: Correlation between ADC/ CBV and quantitative CMRO₂ employing dynamic ¹⁷O MRI
2. Yanis Taege, Johannes Fischer, Ali Özen, Hao Song, Christian Schuch, Rianne Schutter, Cyril Moers, Ronald Borra, Michael Bock; Protocol Optimization for Functional ¹⁷O-MRI of Donor Kidneys at 3T
3. Victor Schepkin, Shannon Helsper, Cathy Levenson; Limitation of glucose consumption in rat head detected by labeled glucose-¹⁷O
4. Yifan Zhang, Yuchi Liu, Kui Xu, Ciro Ramos-Estebanez, George Farr, Joseph LaManna, Walter Boron, Xin Yu; Oxygen-17 MRI Reveals Unchanged Cerebral Metabolic Rate in Aquaporin-4 Knockout Mice

Further publication about Oxygen-17 can be found on our website: nukem-isotopes.de/media

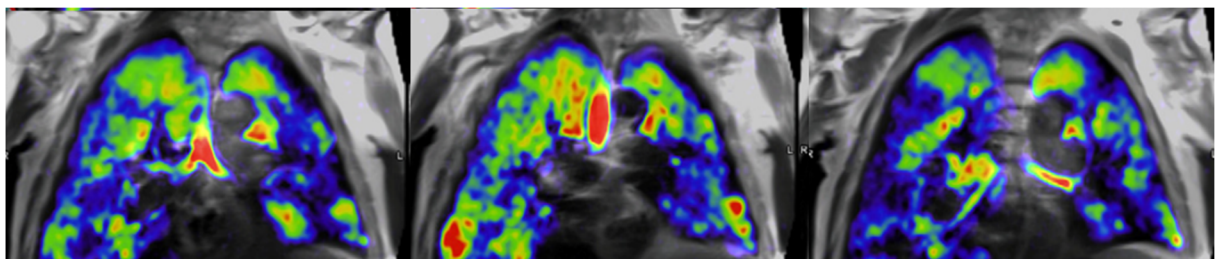


Our cooperation partner - Polarean

Visualization of Lung Function with ^{129}Xe MRI



Visit Polarean at the *2022 The International Society for Magnetic Resonance in Medicine*, Booth F26.



<https://polarean.com/>

Our ISMRM rubber duck family

Due to the great interest in our rubber ducks, we are pleased to introduce our ducks from the previous ISMRM conferences.

The ducks are not for sale and only available at our booth.

*Come and visit us at our ISMRM booth D16 to pick up your **2022 duck**.*



Paramedic **Ben**

London 2022

Our ISMRM rubber duck family



Dr. Jacques

Montreal 2019



Dr. Amy

Paris 2018



Nurse Xenia

Hawaii 2017



Nurse Gudrun

Singapore 2016



Dr. Willy

Toronto 2015



Nurse Alberta

Salt Lake City 2013



Nurse Roberta

Melbourne 2012



Dr. Bob (Robert)

Montreal 2011

NUKEM Isotopes GmbH

Rodenbacher Straße 47
63755 Alzenau, Germany

T +49 (0) 6023 9474 800

F +49 (0) 6023 9474 813

E info@nukemisotopes.de

www.nukemisotopes.de